JOURNAL OF MATERIALS SCIENCE 31 (1996) 6043–6053

Surface modification of an aramid fibre treated in a low-temperature microwave plasma

U. PLAWKY*
Gerhard-Mercator-Universität, Labor für Angewandte Physik, D-47048 Duisburg, Lotharstraße 1-21, Germany

M. LONDSCHIEN
HT TROPLAST AG, D-53840 Troisdorf, Kaiserstraße, Germany

W. MICHAELI
Institut für Kunststoffverarbeitung, an der Rheinisch-Westfälischen Technischen Hochschule, D-52062 Aachen, Pontstraße 49, Germany

The surface modification of an aramid fibre treated in a low-temperature microwave (mw) plasma was investigated. Three different plasma gases, oxygen, argon and ammonia, were used to achieve different surface modifications during fibre treatment. The modification of the fibre surface was analysed with electron spectroscopy and electron microscopy. The influence of the surface modification on the fibre–matrix interaction was inspected by measuring the interlamellar shear strength of the composites and the pull-out strength of a fibre bundle in model composites. The process gas and thus the kind of plasma has no significant influence on the fibre modification resulting from plasma treatment. It was shown that a fibre cleaning with subsequent surface ablation is the dominate modification process during mw plasma treatment, independent of the process gas. The degree of surface cleaning and removal of a contamination layer strongly depended on the treatment range. No incorporation of oxygen or nitrogen containing functional groups was observed. This was explained with the composition of the process gas. The improvements of the composite properties demonstrate the advantage of the mw plasma treatment as a fast, environment-protected, cost-efficient process for fibre modification.

1. Introduction

A controlled modification of the surface of polymer fibres is one of the major aims in composite material sciences. Often the fibre surfaces were treated wet chemically not only to achieve a better processability but also to adjust the fibre matrix adhesion for special purposes such as high strength of the composite or good impact resistance. Therefore, special coupling agents were developed to achieve optimum properties for given fibre matrix systems. The tailoring of coupling agents is a great task in chemical research and material science because a controlled strength of adhesion interrelates constitution, morphology, rheology and processing characteristics of reinforced composites [1–3]. Additionally, the research on new high-performance polymer fibres for technical applications leads to the need for new coupling agents besides, for example, the established research on silane couplings agents for the E-glass fibre industry. In addition to the traditional way of wet-chemical treatment of the fibre surface, in the last years some new methods for surface modification have been established.

One way to modify polymer surfaces and thus tailor the interphase between composites, is the low-temperature plasma treatment (e.g. [4–6]). Depending on the plasma process technique, several ways of surface modification are possible. These are, for example, surface activation, surface cleaning and/or changing of surface texture. The kind of treatment depends on the activation frequency for the process gas, the process gas itself (e.g. inert gases such as argon, or reactive gases such as oxygen), the process pressure and the operation mode. Much research has been performed in this area using different plasmas (different activation frequencies thus resulting in different characteristic plasma parameters), different treatment modes and different construction sets [7–11].

In a previous paper, the surface modification of a polyethylene (PE) fibre in a low-temperature microwave (mw) plasma was investigated [3]. It was shown that an adjustable degree of surface oxidation of the PE fibre could be achieved, depending on the process parameters. Additionally, the incorporation of oxygen in different functional groups could be varied by changing the processing conditions. The resulting high

* Author to whom correspondence should be addressed.

0022–2461

surface oxidation of the fibre due to the plasma treatment greatly improved the fibre–matrix interaction, as was shown by mechanical tests on model composites.

In this work, the influence of a low-temperature mw plasma on the properties of an aramid fibre was investigated. Different plasma gases were used to analyse several possible surface modifications. Argon and oxygen were used as process gases to analyse possible surface cleaning, etching or degradation mechanisms. Additionally, ammonia was used as the process gas to achieve an incorporation of nitrogen-containing functional groups in the fibre surface. The influence of the different surface treatments on the fibre–matrix interaction was analysed using model composites. As mechanical properties, the average interlamellar shear strength and the fibre bundle pull-out strength were determined.

2. Background

According to the definition of the American Federal Trade Commission aramid fibres are made of long-chain synthetic polyamides with at least 85% amide groups linked directly to two aromatic rings. The fibres used in this work consist, like other aramids, of oriented molecules of poly(*p*-phenylene terephthalamide) (PPTA). The PPTA molecules are the result of the polycondensation of terephthalchloride with *para* (phenylenediamine) in a suitable solvent [12, 13].

To understand the structure–properties relationship of aramid fibres, a basic knowledge of the process conditions is important [14–20]. In concentrated sulphuric acid (H_2SO_4) above a critical concentration (in the range of 20 wt % PPTA), the PPTA molecules form a liquid crystalline phase, resulting in an anisotropy of the system (PPTA–H_2SO_4)$_{(liquid)}$. The PPTA molecules show a local order in one direction. The fibre is spun out from the anisotropic solution and the solvent is sprouted off by a water bath. Additional cleaning processes are followed, for example, for neutralization of the sulphuric acid. At least the fibre is dried under tensile strength with subsequent drawing.

The fibre consists of long-chain rod-like molecules, which are oriented along the fibre axis. Owing to the chemical constitution, secondary effects for planar order exist. Molecular chains are hydrogen bonded in the direction of the *b*-axis. Van der Waals forces act between layers in the *a*-axis direction and due to covalent bonds the fibre has high strength in the *c*-axis direction (the fibre direction). Aramid fibres have a low flexibility due to high barriers associated with virtual and amide C–N bonds. A schematic model for the conformation and configuration of the PPTA molecules is shown in Fig. 1. The dotted lines represent the hydrogen bonds.

The fibre morphology is very relevant to its mechanical behaviour. Techniques such as electron microscopy, small-angle X-ray scattering and electron diffraction have revealed a longitudinal and transverse microstructure of the outer skin and inner core and other important features of morphologic details [14, 15, 21–25]. Morgan *et al.* [14] developed a morphology model of the aramid fibre due to correlations between physical properties and deformation-induced failure mechanisms. This model is shown in Fig. 2. The fibre exhibits two phases with different order character. The polymer chains in the fibre skin are preferentially oriented parallel to the surface, in contrast to the radial sheet structure of the core. The rod-like PPTA molecules are parallel to the fibre axis along the fibre diameter. The chain ends in the skin are parallel to each other, or else without any order, and are thus highly axially oriented. The result is a statistical chain-end overlapping in the skin region. Cylindrical crystals in the fibre core are imperfectly packed and ordered, and the chains in these crystallites are aligned parallel to the fibre axis. The chain ends in the crystals are clustered near crystal boundaries. The crystals are linked together by only a few tie molecules. Voids and cavities in the skin or core region are presented due to segregation or diffusion of solvent residuals or other impurities and shrinkage processes.

The above-described skin–core structure of the aramid fibre is a result of the fibre-processing technique. A temperature gradient between inner and outer parts of the fibre during the high cooling rate in the coagulation bath freezes the outer chains before they can crystallize. In the inner region, the cooling rate is low enough to allow crystal formation. This results in several levels of superimposed microscopic

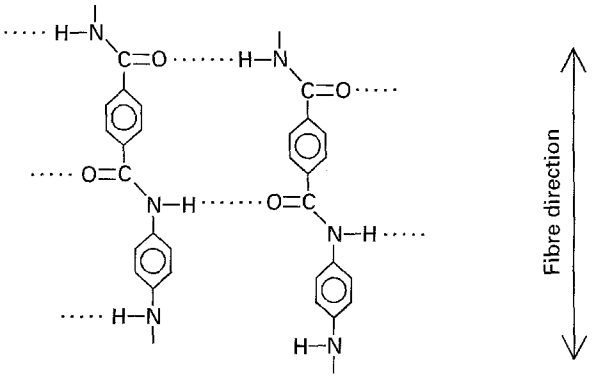

Figure 1 Schematic illustration of the PPTA molecules in the aramid fibre.

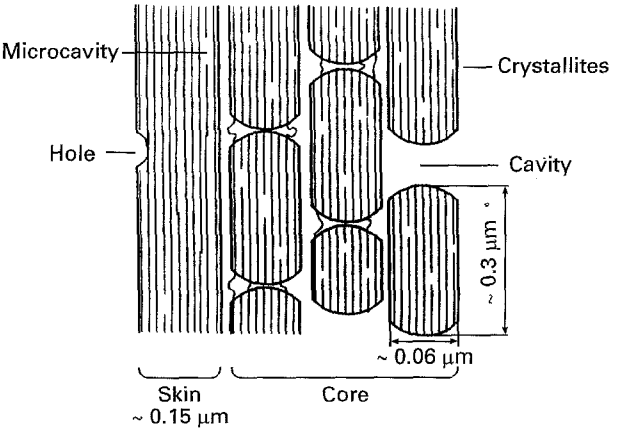

Figure 2 Morphological model of the aramid fibre, after [14].

and macroscopic structure. Also many conformational defects arise, e.g. voids, as defects in the skin structure. Additionally, a contamination layer sticks to the fibre surface. It consists mainly of oxidized hydrocarbons [14].

From the above-described morphology, interesting but also disadvantageous application properties arise. Aramid fibres have a high specific strength, show a high temperature resistance and excellent resistance to chemical environments. Under compression, the fibre exhibits buckling. In bundles used in composites, these effects may be intensified by weak fibre–fibre or fibre–matrix interactions due to bad load transfers across an ineffective interphase. The occurrence of internal instability at low stress levels has been explained in terms of high mechanical anisotropy of the fibre. Failure regions show a high degree of interfacial debonding and fibrillation [19]. Besides this, aramid fibres show favourable impact properties. Many studies on analysing and improving the aramid–matrix interface effects were made to overcome the above-mentioned drawbacks (see, for example, [26–32]).

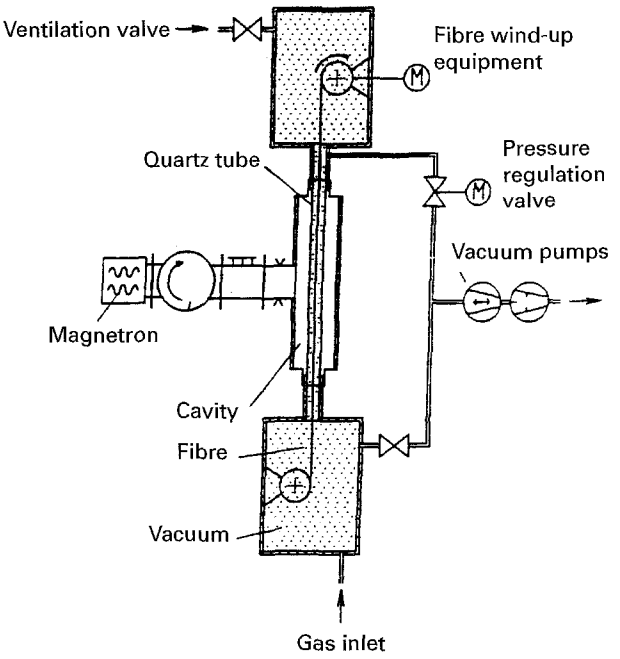

Figure 3 Schematic drawing of the construction set for fibre treatment [34].

3. Experimental procedure

3.1. Materials

In this presentation, an aramid fibre, Twaron© 1055 from Akzo, Arnhem, The Netherlands, was investigated [14]. The fibre surface was treated wet-chemically by the supplier to improve the fibre processability. Small droplets of undisclosed composition were spread inhomogeneously over the fibre surface, the amount of surface modification lying in the range of 1% by weight. The fibre was used as-received from the supplier; no surface cleaning or any other treatment was performed before treatment in a low-temperature plasma.

3.2. Fibre treatment

3.2.1. Plasma reactor and process parameters

The plasma reactor used in this investigation is a pilot construction especially made for fibre treatment and designed at the Institut für Kunststoff-Verarbeitung (IKV) an der Technischen Hochschule Aachen, Germany. It is schematically shown in Fig. 3. The complete construction is described in detail elsewhere [3, 33, 34]. It consists of two recipients arranged vertically to one another and connected by a quartz glass tube. The untreated fibre is placed in the lower chamber and can be wound up into the upper chamber. The chambers are sealed against atmospheric pressure and a controlled vacuum can be adjusted during the process. A cavity (the resonator) surrounds the quartz tube. For the excitation of the process gas, a microwave generator was used operating at the frequency of 2.45 GHz. The output power could be adjusted from 120–1200 W. A gauge meter is installed in the waveguide line to determine the power dissipated in the system. The system consists of the active length of the quartz tube, the resonator and the process gas. As process gases, argon, oxygen and ammonia were used.

The homogeneity of the plasma was controlled optically along the quartz tube and across the tube diameter, respectively. As a control parameter, the spatial distribution of the plasma intensity across the tube diameter was observed visually. The spatial distribution of the microwave field in the plasma reactor was adjustable by varying the active length of the cavity with Teflon plates and by varying the active length of two antennae perpendicular to the cylinder axis. For every set of process parameters, the homogeneity of the plasma was controlled to impart a reproducible treatment of the fibres.

Measurements revealed that the absorbed mw power is proportional to the input power and nearly process-gas independent. This is shown in Fig. 4 for all process gases. No dependence on other parameters was observed. Without active plasma, nearly the whole input power is reflected, thus showing that only the process gas absorbed the mw energy [34]. Most of the absorbed mw energy is re-emitted through relaxation effects of the excited gas which acts as an intense ultraviolet radiation source. Nearly the whole re-emitted radiation is absorbed by the quartz tube which heated up to high temperatures [3, 34, 35].

Analysis of the gas composition of the process gases was done with mass spectroscopy. These measurements were performed on an equivalent construction set designed for plasma treatment of samples with arbitrary geometry [33]. The process parameters were an active gas flux of 50 standard cm^3min^{-1} (1 cm^3 process gas at normal conditions per minute) and a pressure of 50 Pa. As an example, the gas composition of oxygen as process gas is shown in Fig. 5. For all process gases, a high amount of water is presented. Using argon or ammonia, the amount of water is in the range of 20% and 15%, respectively [35].

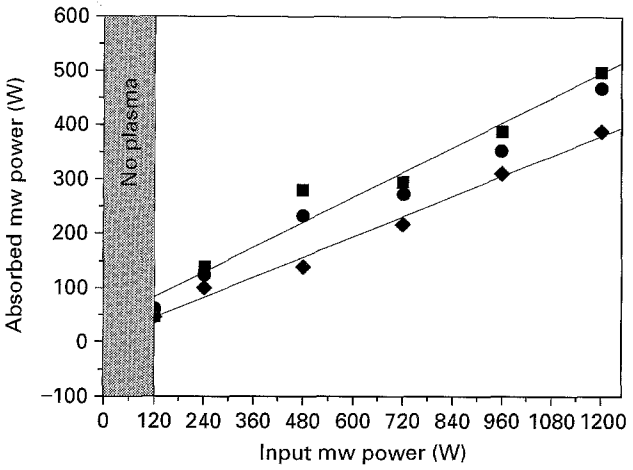

Figure 4 Absorbed microwave power using different process gases: (□) O_2 plasma, (○) argon plasma, (◇) NH_3 plasma; the lines represent the upper and lower limits.

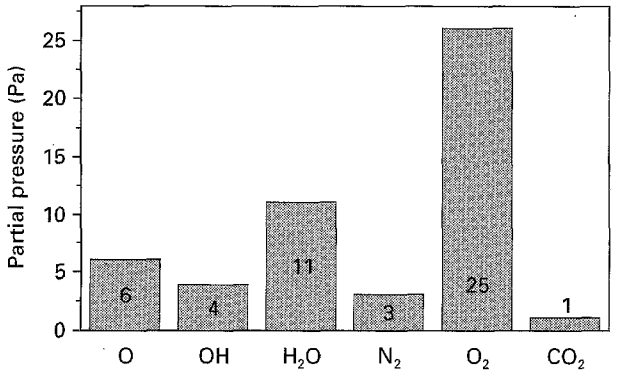

Figure 5 Gas composition at typical process conditions: oxygen flux of 50 standard cm^3min^{-1} and a process pressure of 50 Pa.

3.2.2. Treatment range

Besides the design of the construction set for the plasma treatment and the properties of the plasma, the treatment range is limited by the energy absorption of the fibre. Due to the plasma treatment, the fibres were heated up. This rise in temperature has two origins. First, the plasma as source of a particle flux and ultraviolet radiation leads to a direct heating of the fibre. Second, the fibre is heated up by the temperature radiation of the surrounding quartz tube. The thermal stability of the fibre is therefore the critical factor for the process range.

The treatment range was determined by measuring the tensile strength of the fibres after treatment in an oxygen plasma and comparing the results with those of the untreated fibre [36]. The process parameters, which show no deterioration in the mechanical fibre properties define the treatment range. The mw input energy into the system and thus the activation energy for the plasma is given by the treatment time and mw input power. The mw energy input for fibre treatment was in the range from 12–600 J. Throughout this investigation, a process pressure of 50 Pa and a process gas flux of 50 standard $cm^3\ min^{-1}$ were used as standard parameters.

The treatment of the fibres took place in a batch mode. First the fibre was put into the lower chamber and the construction was evacuated to the minimum pressure to avoid any mistakes during the process by hidden leaks. The minimum pressure reached with the vacuum pumps was in the range of 0.1 Pa at 0 standard $cm^3\ min^{-1}$ active gas flux. After adjusting the process parameters, the mw generator was switched on and the plasma was verified for homogeneity. The fibre was wound up at a known velocity and thus moved through the plasma for a known treatment time. After spooling up the fibre, the mw generator and the pumps were switched off and the chambers were ventilated [3].

3.3. Characterization techniques

3.3.1. Electron spectroscopy for chemical analysis

The characterization of the fibre surface modification was performed by electron spectroscopy for chemical analysis (ESCA). This technique is a surface-sensitive method to determine the elements (with the exception of elementary hydrogen) and their binding states on the surface [37–39]. Different binding states of an atom, e.g. carbon in functional groups with oxygen, result in different binding energies, compared to for example, a pure carbon–carbon bond. This difference in binding energy, called the shift in binding energy (ΔBE), of the observed element is a measurable quantity and can give further information about the chemistry of the investigated surface [40–45].

Throughout this investigation, a computer-controlled Small Spot M-Probe from Surface Science Instruments (SSI M-Probe), operating with monochromatic X-ray radiation of the line was used for the ESCA measurements. This spectrometer has a high lateral resolution and a flood gun to prevent charging effects of non-conducting samples like polymers [3, 35, 46, 47].

From each treated fibre bundle, five small pieces (a few centimeters long) were cut off and different locations on the surface were analysed in two steps. First a survey scan was recorded to examine the elemental composition of the surface. This gave a value of the total amount of element X (e.g. oxygen) on the fibre surface. A high-resolution spectrum of carbon, oxygen and nitrogen (C 1s, N 1s and O 1s spectrum, respectively) was measured to estimate the binding states in the fibre surface. In this investigation, the C 1s binding energy of the graphite peak (the pure C–C bond) was taken as 285.0 eV. This value is often used as a binding energy reference [37]. In other investigations, a value of 284.6 eV for calibration purposes was used [48].

In the analysis and quantification of surface functional groups, the various proportions of carbon functional groups containing oxygen or nitrogen have been determined by applying a computer curve fitting technique to the carbon C 1s spectrum (see, for example, the work of Sherwood and co-workers [48–53] concerning this technique). The curve fitting was carried out by using a non-linear least-squares curve-fitting program with a Gaussian–Lorentzian

product function [47]. The fitted parameters could yield start values with constraints, so variations only in small intervals were possible. These boundary conditions were necessary to keep the resulting envelope of the fit to the measured curve.

Besides the aramid fibre, additional measurements on model molecules were performed to investigate the influence of oxygen- or nitrogen-containing functional groups on the shift in binding energy of carbon. These molecules were terephthalic acid, 4-aminobenzoic acid and 4-aminobenze amide. Their high-resolution spectra (C 1s, O 1s and N 1s) were recorded for comparison with the high-resolution spectra of the aramid fibre. A deconvolution of the high binding energy shoulder on the measured C 1s peak of both the aramid fibre and the model molecules, gave several peaks which can be ascribed to the following functional groups:

(i) group I, $-CH_2O-$ (e.g. alcohol, ether, ester, hydroperoxide) with $\Delta BE \approx 1.6$ eV;

(ii) group II, $>C=O$ (e.g. aldehyde, ketone) with $\Delta BE \approx 2.9$ eV;

(iii) group III, $-CO_2R$ (e.g. carboxylic acid/ester) with $\Delta BE \approx 4.1$ eV.

These three groups overlap with possible nitrogen-containing functional groups which can be ascribed to:

(a) group I_a, $C-NH_2$ (e.g. amide functionalities) with $\Delta BE \approx 1.6$ eV, or

(b) group II_a, $O=C-NH_2$ (e.g. amine functionalities) with $\Delta BE \approx 2.6$ eV.

The measured values for the shifts of the binding energies (ΔBE) were in good agreement with literature results (see, for example [37, 51, 54]). The above proposed functional groups should be regarded as representative functional groups [37]. These values were used to characterize the chemical composition of the surface of both treated and untreated fibres.

The peak widths of the C 1s peaks of the aramid fibre were much broader, compared to the peak width of the test molecules. A clear distinction between nitrogen- or oxygen-containing functional groups was not possible. Additionally, the contamination layer on the fibre surface made a quantitative and qualitative chemical characterization of the surface more difficult [13, 14].

3.3.2. Electron microscopy

With scanning electron microscopy (SEM), the influence of the plasma treatment on the fibre surface topology was investigated. Therefore, the fibre bundles were fixed on sample holders with a special carbon emulsion. After evaporation of the solvent, the fibres were coated with a thin gold film to prevent charging effects. The electron microscopic investigations were performed on a Leitz AMR 100 which was combined with an energy dispersive X-ray analysis equipment (EDX) to analyse locally (1 μm^2 area) the elemental composition (only elements with higher order number than sodium) of the observed area [39].

3.3.3. Mechanical tests

A possible deterioration of the mechanical properties of the fibre through the plasma treatment was analysed by a tension test after ASTM D 885 M [36]. With these results, the treatment range for the mw plasma treatment was determined (a significant deterioration of the mechanical properties after plasma treatment in between the treatment range was not detected. The Young's modulus was slightly below the specification value of 115 GPa).

The influence of the surface treatment on the fibre–matrix interaction was investigated using the three-point bending test. With this experimental set-up, the interlamellar shear strength (ILS) can be determined [55]. To prepare the composites, a commercial resin system Araldite© Ly 556 was used [56]. The test specimens were cut off the composites plates using a special laser-beam cutting technique [34]. Additionally, fibre bundle pull-out tests were performed to determine the pull-out strength of the model composites. This method is described in detail elsewhere [3].

3.3.4. Other methods

Thermogravimetric analysis (TGA) was performed to determine the weight per cent portion of the droplets (due to the wet-chemical treatment) on the fibre surface.

4. Results and discussion

The main effect of the mw plasma treatment is a surface cleaning with subsequent surface ablation. This could be observed with the SEM. Outside the treatment range (mw input energy of $\geqslant 600$ J), damage of the fibre occurred, independent of gas type. The outer filaments of the fibre bundle changed colour to brown. With slightly higher mw input energy, the amount of brown filaments increased rapidly and the fibre strength decreased significantly. ESCA analysis revealed a strong increase of carbon content of about 10 at % coupled with the changed colour of the fibre. This decomposition process is independent of gas type; thus the ablation process seems to be independent of the chemical processes in the plasma.

The SEM observations for the degradation process indicate that the limit for the fibre treatment is given by thermal effects. At too high temperatures, a carbonization of the fibre takes place. Morgan and Allred give the critical fibre temperature for thermal decomposition and carbonization in the range of 648 K.

The surface structure of the untreated fibre, revealed by the SEM, is shown in Fig. 6. The fibre has a smooth surface without any significant texture. The wet-chemical modification is distributed inhomogeneously over the fibre surface in the form of small droplets. Some defects are observed, these are, for example, holes in the fibre and small grooves due to the spinning process. The holes have diameters of about less than 1 μm (see also Fig. 2).

The process gas and thus the kind of gas plasma have no significant influence on the fibre modification.

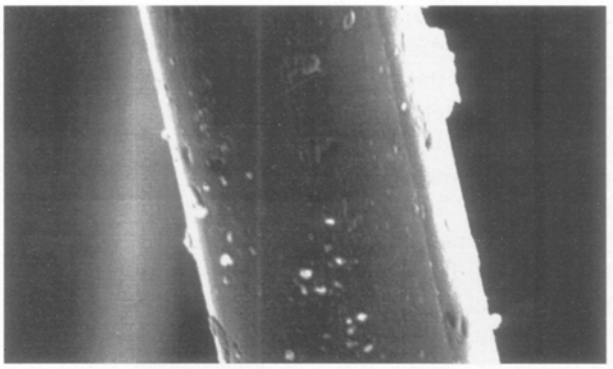

Figure 6 Scanning electron micrograph of the untreated aramid fibre: fibre diameter = 12 μm.

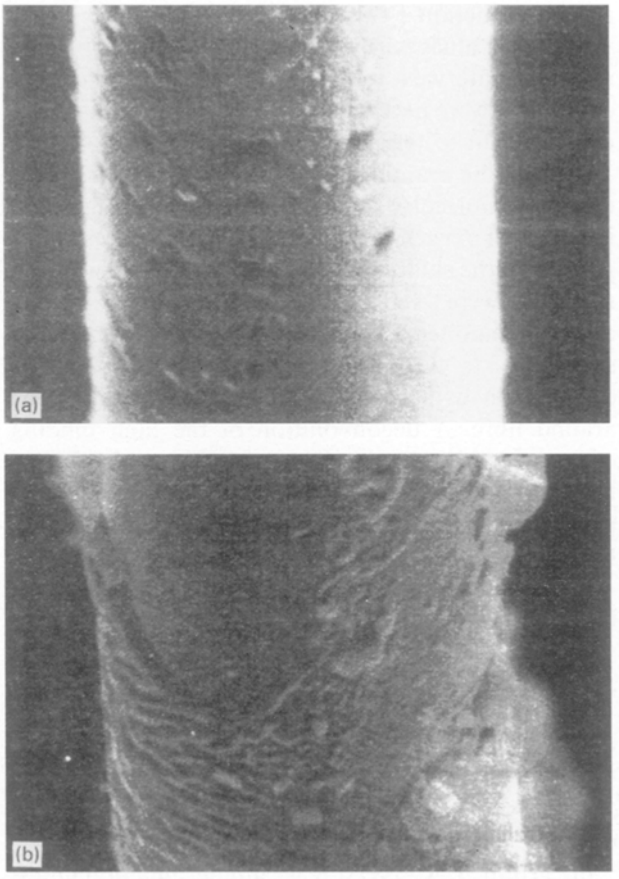

Figure 7 Scanning electron micrograph of a treated aramid fibre: fibre diameter = 12 μm; process parameter: O_2-plasma, 50 standard $cm^3\ min^{-1}$, 50 Pa (a) Microwave energy input 12 J, surface cleaning and etching. (b) Microwave energy input 360 J, surface etching with subsequent ablation.

The fundamental phenomena of the surface variations of the fibre due to plasma treatment are nearly the same for all plasma gases. At low mw energy input, a surface cleaning with subsequent surface ablation is observed. This surface ablation started at defects on the fibre surface, i.e. holes, and depends on the mw input energy.

As an example, the results of an oxygen plasma treatment with standard processing parameters are given in Fig. 7. Fig. 7 shows the result of the plasma treatment with low mw energy input (in the range 12–90 J). The droplets on the fibre surface are removed and the holes on the surface are becoming larger. Microwave energy inputs in the range of 300 J result in local ablation of fibre skin. This is shown in Fig. 7. A surface etching is observed, resulting in local surface ablation. The fibre surface reveals some roughening. Near the treatment limit, ablation of great surface areas of the outer filaments of the fibre bundle is noticed. The described surface modifications are also observed with NH_3 and argon as process gases. Their occurrence is shifted towards higher energy values, i.e. the local surface ablation density with NH_3 as process gas is slightly lower than with oxygen at the same energy value.

The modification of the fibre surface composition was analysed with ESCA. The surface composition of the untreated fibre is different from the expected one due to the chemical structure formula of the fibre. These deviations are the result first from the wet-chemical treatment of the supplier and second from the above-mentioned contamination layer. As mentioned earlier, the contamination layer consists mainly of oxidized hydrocarbons [13]. The oxygen content is twice the value expected for a neat PPTA surface. The measured nitrogen concentration is nearly negligible.

Besides carbon, nitrogen and oxygen, additional contaminations such as silicon, and solvent residuals such as sodium and sulphur, were detected. With the exception of the silicon content, the amounts of these contaminations were in the range of less than 1% and not further considered in this investigation. The silicon content was in the range of 4% relative to 100% carbon, oxygen and nitrogen on the surface. Besides the silicon resulting from the wet-chemical treatment of the supplier, the origin of this contamination was seen in the formation of SiO_2 or abrasion of the quartz tube due to the plasma treatment. Because of the constant amount of silicon, independent of the process parameters, this contamination was neglected in further investigations. EDX analysis revealed some features of the commercial wet-chemical treatment. The droplets have a higher concentration of inorganic elements than the surrounding fibre surface, i.e. potassium, silicon and carbon. Other investigations (e.g. [13, 26]) gave a detailed list of contamination and residual elements using mass and emission spectroscopy.

Throughout this investigation, an elemental composition on the basis of 100% carbon, oxygen and nitrogen on the fibre surface was taken for the quantitative analysis of the ESCA results. Fig. 8 gives the ESCA results of the untreated fibre. For comparison, the expected ESCA values due to the chemical structure of the aramid fibre are also shown. The fibre surface has a significantly higher oxygen concentration as expected. The deconvolution of the Cls peak revealed that oxygen is bound in carbon functionalities. Mainly functionalities of group I, i.e. hydroxyl groups, were calculated by the peak-fitting procedure. This is in agreement with the proposed composition of the contamination layer [14]. Additionally, small amounts of functionalities of groups II and III, i.e. aldehydes, ketones or carboxyls have been resolved by the non-linear curve fitting [47]. The portion of nitrogen-containing functional groups, summarized in

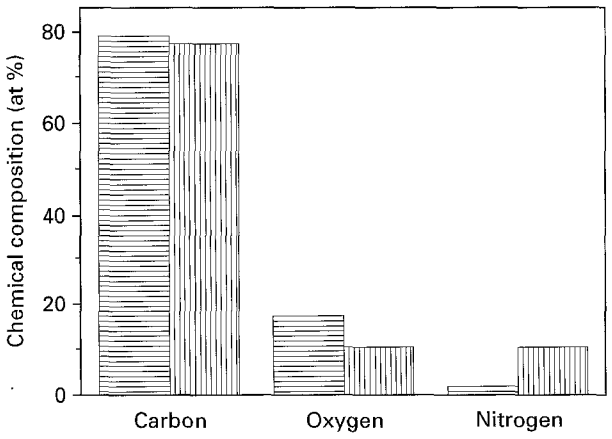

Figure 8 Characterization of the untreated fibre. Comparison of the fibre surface composition after ESCA measurements with the expected surface composition. horizontal lines, experimental values, vertical lines, expected values.

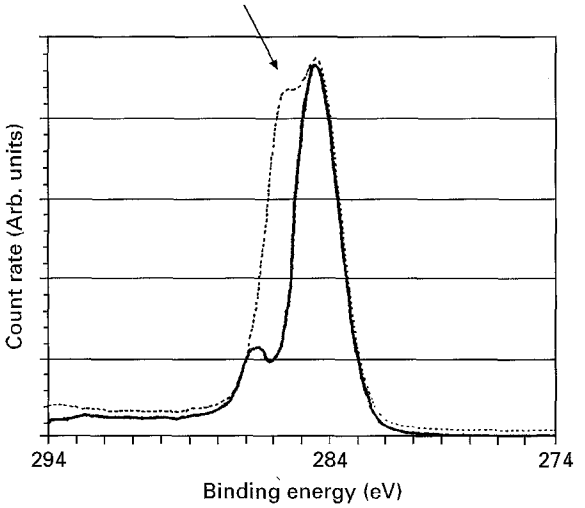

Figure 9 Cls peak of the untreated aramid fibre: (——) fibre as-received, (- - -) purified fibre, after [57]; the arrow indicates the so-called contamination peak.

groups I_a and II_a is still negligible due to the small amount of nitrogen on the fibre surface. This is an indication that the contamination layer covered the complete fibre surface. Its influence on the fibre modification is shown in Fig. 9. Here, the C ls peaks of the untreated fibre and of a fibre without a contamination layer, are presented in the same figure. The removal of the contamination layer was done by a wet-chemical cleaning procedure [57]. A deconvolution of the high binding energy shoulder of the C ls peak revealed that the signal due to the contamination layer is in the range of the shifts in binding energy of the functional groups mentioned earlier. The intensity of the so-called contamination peak (indicated by an arrow in Fig. 9), is used as a quantity to characterize the fibre surface, e.g. the degree of surface coverage of the fibre due to the presence of the contamination layer.

The chemical surface composition of the fibre revealed no significant variation after plasma treatment. This is shown in Figs 10 and 11 for all process gases. In the oxygen plasma at low mw energy input, the carbon concentration decreases and the oxygen concentration increases. With increasing mw energy input, the oxygen content decreases to the value of the untreated fibre and the carbon content increases, the end value staying below the carbon concentration of the untreated fibre. The nitrogen concentration increases only slightly with increasing mw energy, reaching an end value of approximately 4%. Additionally, the contamination peak decreases with increasing mw energy input (as shown in Fig. 11).

At all process parameters, sodium, sulphur or other inorganic contaminations were not further detectable with ESCA. This is an indication that the former wet-chemical treatment of the fibre was removed by the plasma treatment. This was verified with TGA. After a plasma treatment, no residuals of the wetchemical treatment were detectable.

Nearly the same effects on the chemical composition were observed using NH_3 or argon as process gases (see Figs 10 and 11). At low and medium mw energy input, the oxygen content increases. Further increase of mw energy input leads to a decrease of the oxygen content on the fibre surface. The carbon concentration decreases with minimum mw input energy but with increasing mw energy input, its concentration does increase. Additionally, with increasing mw energy input, a slight increase in nitrogen concentration is measured. For minimum mw energy input, the intensity of the contamination peak increases and decreases with further increase of mw energy.

An explanation for the higher oxygen concentration on the fibre surface after treatment in either an argon or ammonia plasma, compared to the pure oxygen plasma is given by Liston [58]. The ultra violet radiation of oxygen in a gas mixture (e.g. Ar/O_2 mixture) is ten times higher than in a pure oxygen plasma. This higher intensity is a result of the frequent dissociation of the oxygen molecules due to the collisions with argon atoms. Because of the chosen process pressure range, in both process gases, ammonia and argon, a high amount of H_2O is present. The activated molecules could dissociate and initiate the oxidation processes.

The results of the surface composition are in good agreement with the formerly described SEM observations. The degree of surface ablation is in correlation with the decrease of the contamination peak. Parallel to the surface cleaning with subsequent surface ablation, the nitrogen concentration on the fibre surface increases. No further evidence of inorganic contaminations was detectable with ESCA, in correlation with the surface topology observed with SEM.

The ESCA results indicate that an amination of the fibre surface has not been achieved. As supported by Figs 10 and 11, an incorporation in nitrogen-containing functional groups has not occurred. The small increase in nitrogen on the surface after the plasma treatment can be explained by cleaning and surface ablation processes. This is in accordance with the decrease of the contamination peak. The low nitrogen content on the surface and the variation of both the oxygen content and the contamination peak on the mw input energy, support this interpretation. The increase of the signal of the contamination layer for low mw energy input with NH_3 and argon as plasma gases, coupled with the increase of oxygen on the fibre

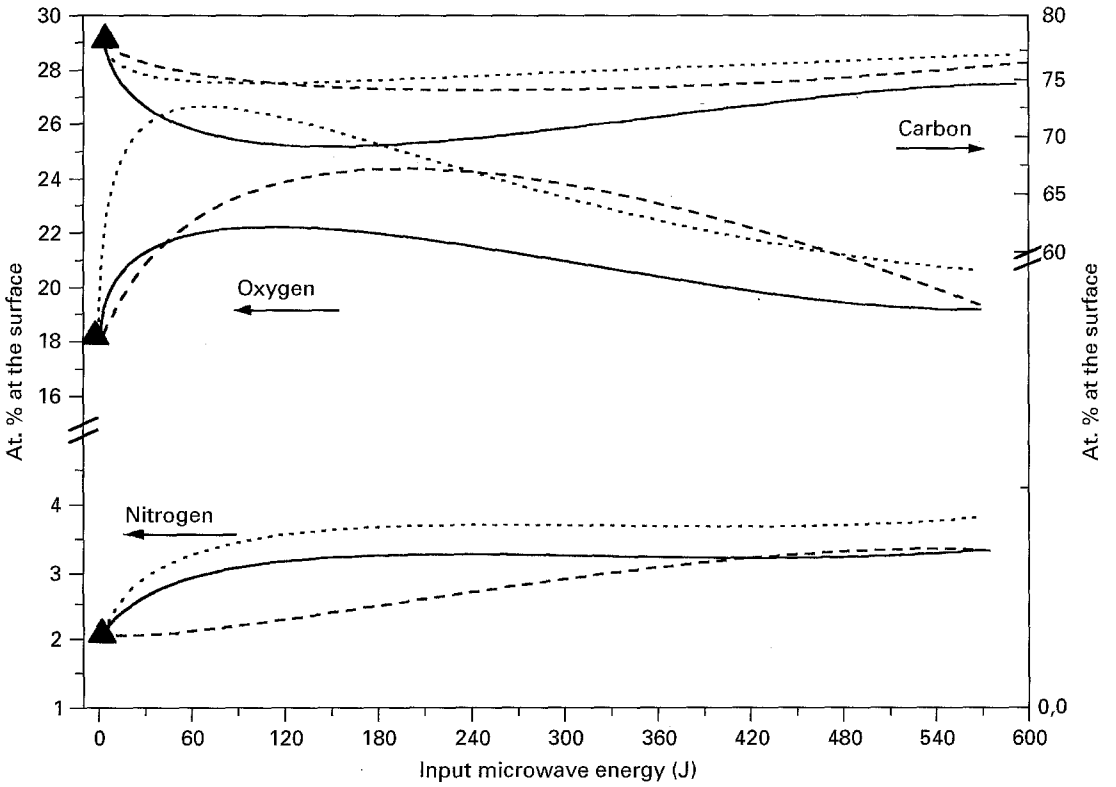

Figure 10 Surface composition of the aramid fibre after plasma treatment: (—) O_2 plasma tendency, (- - -) argon plasma tendency, (...) NH_3 plasma tendency.

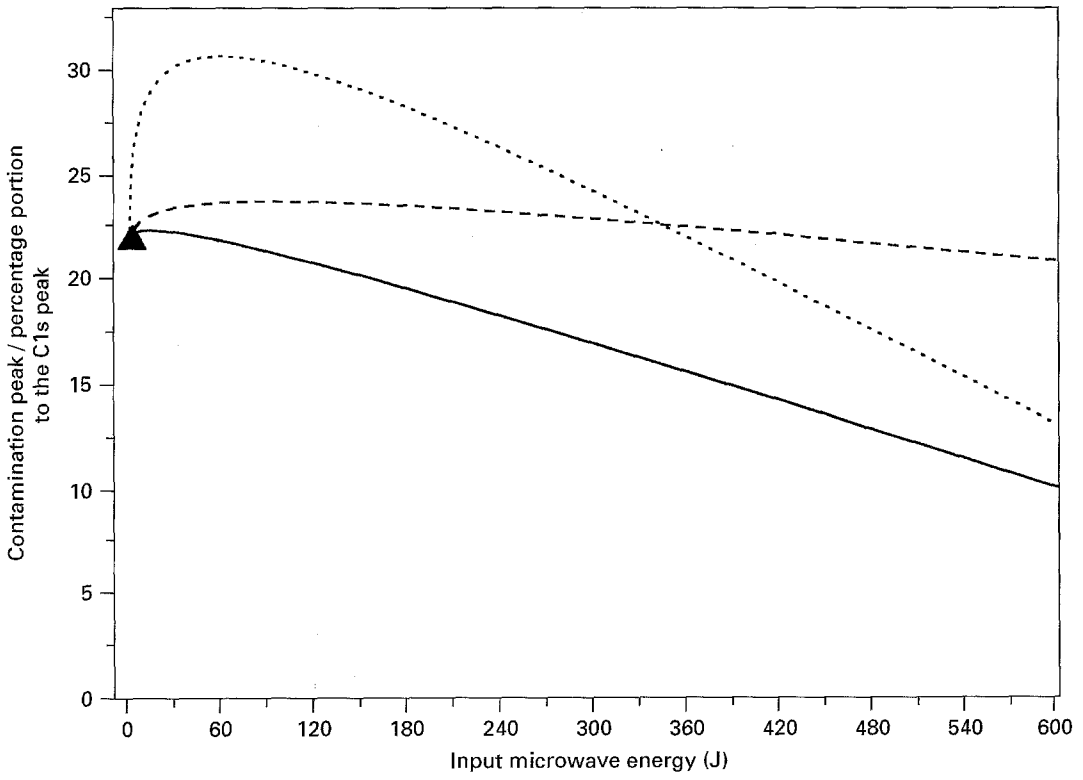

Figure 11 Dependence of the contamination peak on treatment gas and mw input energy: (—) O_2 plasma tendency, (- - -) argon plasma tendency, (...) NH_3 plasma tendency.

surface, is an indication of an oxidation process rather than incorporation of nitrogen on the fibre surface. Two mechanisms can explain the suppression of the surface amination of the aramid fibre. The characteristic features of the mw plasma in the presented experimental set-up are the presence of water in the residual gas composition and the intense ultra violet radiation. Morgan and Allred [13] mentioned that the aramid fibre is partially damaged due to hydrolysis and photodegradation processes. These observations are

supported by Carlsson *et al.* [59]. The chemical reactions, initiated by both phenomena, could suppress a possible incorporation of nitrogen into the fibre surface.

To investigate the influence of the mw plasma treatment on the fibre–matrix interactions of model composites, standard test specimens were prepared using a commercial epoxy resin system [56]. The ILS of the composite was determined following DIN EN 2653 [55]. The values of the ILS as a function of the input mw power are given in Fig. 12 for fibres treated in an oxygen plasma with standard process parameters (50 standard $cm^3 min^{-1} O_2$ flux, 50 pa, 0.1 s treatment time and increasing mw power). For comparison, the ILS values of a composite with a special wet-chemical treated aramid fibre (Twaron© 1058 [12], treated by the supplier for improved interactions with epoxy resin systems) and the reference value of the untreated fibre (only with the processing aid) are also shown in Fig. 12. A treatment of the fibre with minimum mw energy increases the ILS value compared to the value of the untreated fibre and also to the ILS improvement of the commercially treated fibre. As supported by SEM and ESCA results, at this low mw energy input, the fibre is cleaned and the removal of the contamination layer started (cf. Fig. 7a). This explains the improvement of the strength of the fibre matrix interface [60, 61]. With increasing input energy, the ILS of the composites decreases, reaching ILS values in the range of the untreated fibre. In this range, in addition to cleaning of the fibre surface and removal of contamination, additionally ablation of the fibre skin began. The maximum improvement ($\approx 12\%$) is reached at low mw energy input, which can be achieved at short treatment times (0.1 s) and so, therefore, high treatment velocities (in the range of $\geqslant 100\ m\ min^{-1}$, depending on the spool diameter of the fibre winding set-up). This is important if one takes into account the production velocity of the aramid fibre, which is in the range of $300\ m\ min^{-1}$ [62].

Several other authors also deal with a treament to modify the surface of the aramid fibre [29–32, 59, 62]. Wertheimer *et al.* [62] used several process gases (e.g. ammonia, argon) to modify the aramid fibre surface in a mw plasma. They, too, observed a roughening of the surface due to oxidation processes. Allred *et al.* [29, 31] investigated the influence of a radio frequency (r.f.) plasma for fibre surface modification. An increase of 30% in the interlamellar shear strength due the treatment was achieved. Additionally, an incorporation of nitrogen into the fibre surface after plasma treatment was observed, increasing the surface concentration to 14% N. A roughening of the surface was not noticed [29]. Penn *et al.* [32] inspected the influence of a former wet-chemical fibre cleaning procedure on the surface modification in a r.f. plasma with monomethylamine as process gas. A subsequent wet-chemical process incorporated additional functional groups on the fibre surface. The chemical modification of the fibre without change of surface texture resulted in no improvements of composite properties. Wu and Tesoro [30] investigated a wet-chemical surface modification with nitrogen or bromine-containing functional groups. A 50% improvement of the interlamellar shear strength of the composites was achieved with the modified fibre.

In this presentation, the surface cleaning with subsequent slight surface etching increases the ILS of the composites at about 12% thus revealing an improved fibre–matrix interaction. This was proved with a second test method, the fibre-bundle pull-out test, described in detail elsewhere [3, 34]. The results are shown in Fig. 13. The fibre-bundle pull-out strength of the untreated fibre, the special wet-chemical treated fibre and of the fibre treated in an oxygen plasma, are shown. The resin system was the same as for the ILS specimens. The parameters for the O_2-plasma treatment were a gas flux of 50 standard $cm^3 min^{-1}$, a process pressure of 50 Pa, a treatment time of 0.1 s and an mw input power of 120 J. The improvement of the pull-out strength of the fibre treated in the

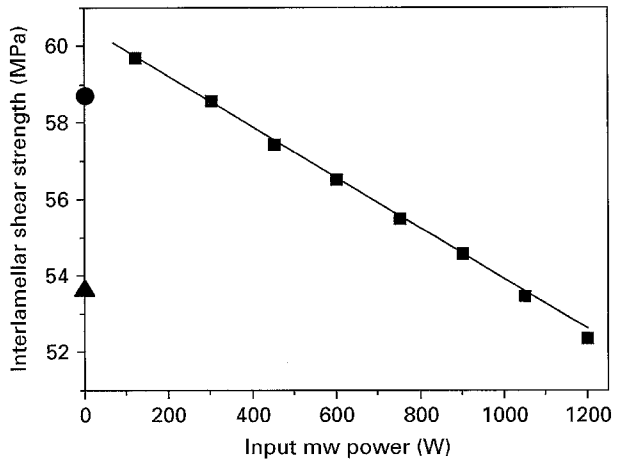

Figure 12 Interlamellar shear strength of composites of O_2 plasma-treated aramid fibres with standard process parameters: (△) untreated fibre, (○) wet-chemical treated fibre, (□) O_2 plasma-treated fibre.

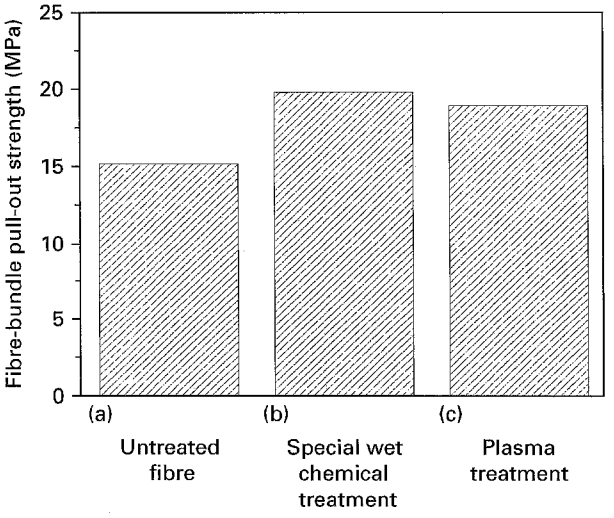

Figure 13 Comparison of the fibre-bundle pull-out strength of aramid fibres in epoxy resins: (a) no treatment, (b) special wet-chemical treatment, (c) O_2 plasma treatment.

oxygen plasma is in the range of the special wet-chemical treated fibre thus verifying the improvement of the fibre–matrix interaction after mw plasma treatment.

5. Conclusion

It is concluded that the concept of the plasma treatment for modifying fibre–matrix properties to improve the composite performance is successful in substituting the complicated and time-consuming wet-chemical modification techniques. The advantages of the plasma treatment are the uncomplicated processing technique, the dry environment-protected process, short treatment times and, therefore, high treatment speed. This makes the mw plasma treatment an interesting and cost-efficient treatment technique for the fibre-processing industry.

After the plasma treatment, the fibre surface is cleaned and loose contaminations are echted off. A former raised processing aid is removed and a slight surface roughening is observed without deterioration of the fibre strength properties. The fibre–matrix interface strength is increased, as was shown by measuring the ILS of test composites, and verified with a second mechanical test method.

Through ablation processes, a local roughening of the fibre surface starts, which ends in fibre destruction through thermal decomposition at too high a mw input energy. An incorporation of nitrogen into the fibre surface through the plasma treatment is suppressed by several other mechanisms which could be prevented with oxygen- or water-free gas mixtures.

References

1. E. P. PLUEDDEMANN, in "*Mechanical Properties of Reinforced Thermoplastics*", edited by D. W. Clegg and A. A. Collyer (Elsevier, London, 1986) 249.
2. F. N. COGSWELL, *ibid.* 83.
3. U. PLAWKY, M. LONDSCHIEN and W. MICHAELI, *Polymer Acta.* **47** (1996) 112.
4. H. VON BOENING, "*Plasma Science and Technology*" (Hanser, München, 1982).
5. A. T. BELL, "*Techniques and Applications of Plasma Chemistry*" (Wiley, New York, 1974).
6. H. DROST, "*Plasmachemie*" (Akademieverlag, Berlin, 1978).
7. "*Interfaces in Polymer, Ceramic, and Metal Matrix Composites*", H. Ishida (ed.), Proceedings of the Second International Conference on Composite Interfaces (ICCI-II), Part 1, p. 1, 1988 Cleveland, OH (Elsevier, New York, 1988).
8. J. B. DONNET, T. L. DHAMI, S. DONG and M. BRENDLÈ, *J. Appl. Phys.* **20** (1987) 269.
9. G. C. S. COLLINS, *Eur. Polym. J.* **9** (1973) 1173.
10. D. J. CARSSON, *J. Polym. Sci. Poly. Chem.* **16** (1978) 2353.
11. M. R. WERTHEIMER and J. E. KLEMBERG-SAPIEHA, *Thin Solid Films* **115** (1984) 109.
12. ANON., "*Twaron Technical Documentation*", AKZO Fibres Arnhem, NL (1985).
13. R. J. MORGAN and R. E. ALLRED, in "*International encyclopedia of composites*", *Vol. 1*, edited by S.M. Lee, (Wiley, New York, 1991).
14. R. J. MORGAN, C. O. PRUNEDA and W. L. STEELE, *J. Polym. Sci. Polym. Phys. Ed.* **21** (1983) 1751.
15. S. C. SIMMENS and J. W. S. HEARLE, *ibid.* **18** (1980) 871.
16. D.C. PREVORSEK, in "*Polymer Liquid Crystalls*", edited by A. Ciferri, W. R. Krigbaum and R. B. Meyer (Academic Press, New York, 1982) 329.
17. E. J. KRENDLINGER *PhD thesis Mainz*, Germany (1990).
18. M. G. NORTHOLT and J. J. VAN ARSEN, *J. Polym. Sci. Polym. Lett. Ed.* **11** (1973) 333.
19. H. W. RAYSON, G. C. McGRATH and A. A. COLLYER, in "*Mechanical Properties of Reinforced Thermoplastics*", edited by D. W. Clegg and A. A. Collyer (Elsevier, London, 1986).
20. Q. ZHANG, Y. LIANG and S. B. WARNER, *J. Polym. Sci. Polym. Phys.* **32** (1994) 2207.
21. R. K. HASEGAWA, Y. CHATANI and H. TADOKORO, in "*Meeting of the crystallographic Society of Japan*", Osaka, Japan (1973) p. 21.
22. K. TASHIRO, M. KOBAYASHI and H. TADOKORO, *Macromolecules* **10** (1975) 524.
23. L. PENN and F. LARSEN, *J. Appl. Polym. Sci.* **23** (1979) 59.
24. M. G. DOBB, D. J. JOHNSON and B. P. SAVILLE, *J. Polym. Sci. Polym. Phys. Ed.* **15** (1977) 2201.
25. M. PANAR, P. AVAKAIN, R. C. BLUME, K. H. GARDNER, T. D. GIERKE and H. H. YANG, *ibid.* **21** (1983) 1955.
26. R. H. ERICKSON, *Composites.* **7**(3) (1976) 189.
27. M. TAKAYANAGI, T. KAJIYAMA and T. KATAYOSE, *J. Appl. Polym. Sci.* **27** (1982) 3903.
28. L. PENN, in "*Adhesia Society, 5th Annual Meeting*", Mobile, AL (1982) p. 22.
29. R. E. ALLRED, E. W. MERILL and K. ROYLANCE, in "*Molecular Characterisation of Composited Interfaces*", edited by H. Ishida and G. Kumar (Plenum Press, New York, 1985) 333.
30. Y. WU and G. C. TESORO, *J. Appl. Polym. Sci.* **31** (1986) 1031.
31. R. E. ALLRED, in "*29th National SAMPE Symposium*" SAMPE Journal Committee (1984).
32. L. PENN, T. J. BYERLEY and T. K. LIAO, *J. Adhes.* **23** (1987) 163.
33. R. LUDWIG, *PhD thesis, RWTH Aachen*, Germany (1988).
34. M. LONDSCHIEN, *PhD thesis, RWTH Aachen*, Germany (1992).
35. U. PLAWKY, Diploma thesis, RWTH Aachen, Germany (1992).
36. ANON., *ASTM D 885 M: Annual book of ASTM standards, Vol. 7.01, "Textiles"*, (American Society for Testing and Materials, Philadelphia, PA, 1985).
37. D. BRIGGS, in "*Practical Surface Analysis*", edited by D. Briggs and M. P. Seah (Wiley, New York, 1985) 359.
38. K. SIEGBAHN, "*ESCA Applied to Free Molecules*" (North Holland, London, 1969).
39. G. KÄMPF, "*Charakterisierung von Kunststoffen mit physikalischen Methoden*" (Hanser, Beuth, München, 1982).
40. L. J. GERENSER, *J. Adhes. Sci. Technol.* **1** (1987) 303.
41. D. T. CLARK, B. J. CROMARTY and A. DILKS, *J. Polym. Sci. Polym. Phys. Ed.* **16** (1978) 3173.
42. D. T. CLARK and A. DILKS, *J. Polym. Sci., Polym. Chem. Ed.* **17** (1979) 957.
43. D. T. CLARK and A. HARRISON, *ibid.* **19** (1981) 1945.
44. D. T. CLARK, in "*Electron spectroscopy – Theory, Techniques and Applications*", edited by C. R. Brundle and A. D. Baker, Vol. 4 (Academic Press, New York, 1981) 278.
45. A. DILKS and A. VAN LAEKEN, in "*Physicochemical Aspects Of Polymer Surfaces*", Vol. 2, edited by K. L. Mittal (Plenum Press, New York, 1983) 163.
46. ANON., in "*M Probe Operator's Manual*" (Surface Science Instruments, 1991).
47. ANON., in "*Software Manual Version 1.3*" (Surface Science Instruments, 1992).
48. C. KOZLOWSKI and P. M. A. SHERWOOD, *J. Chem. Soc. Farad. Trans. I.* **81** (1985) 2745.
49. A. PROCTOR and P. M. A. SHERWOOD, *J. Elec. Spec.* **27** (1982) 39.
50. *Idem, Carbon*, **4** (1982) 212.
51. *Idem, Surf. Interf. Anal.* **27** (1982) 39.
52. C. KOZLOWSKI and P. M. A. SHERWOOD, *J. Chem. Soc. Farad. Trans. I.* **80** (1984) 2099.
53. *Idem, Carbon.* **24** (1986) 357.
54. D. M. BREWIS and D. BRIGGS, *Polymer* **22** (1981) 7.
55. ANON., *DIN EN* 2653 (Beuth, Berlin, 1990).

56. ANON., "*Technical report on matrix systems*" (Ciba-Geigy, Basel, 1980).
57. J. W. G. MAHY, *personal communication*, Akzo Arnhem (1991).
58. E. M. LISTON, *J. Adhes.* **30** (1989) 199.
59. D. J. CARLSSON, L. H. GAN and D. M. WILES, *J. Polym. Sci. Polym. Chem. Ed.* **16** (1978) 2365.
60. J. KALANTER and L. T. DRZAL, *J. Mater. Sci.* **25** (1990) 4186.
61. *Idem, ibid.* **25** (1990) 4194.
62. M. R. WERTHEIMER and H. P. SCHREIBER, *J. Appl. Polym. Sci.* **26** (1981) 2087.
63. E. BRACHES, *personal communication*, Enka Akzo, Wuppertal (1990).

Received 31 October 1995
and accepted 24 April 1996